

## Mechanism of Transition in Magnetite at Low Temperatures\*

H. J. WILLIAMS, R. M. BOZORTH, AND MATILDA GOERTZ  
*Bell Telephone Laboratories, Murray Hill, New Jersey*

(Received May 7, 1953)

When magnetite is cooled through  $-160^{\circ}\text{C}$  it is known to undergo a transition (cubic to orthorhombic) that is influenced by the presence of a magnetic field. Our experiments are in agreement with the following mechanism of the transition: The orthorhombic  $c$  axis is parallel to one of the original cubic axes and is the axis of easiest magnetization. Generally, different regions of the original crystal will transform with their  $c$  axes lying along different cubic axes, and when no field is applied there are 6 different orientations which different regions assume. When a field is applied during cooling a  $c$  axis tends to lie along the original cubic axis that is nearest to the applied field, the  $a$  and  $b$  axes having less but different tendencies to lie parallel to the field.

Six magnetic crystal anisotropy constants are derived from torque curves measured in the (100) and (110) planes. From them magnetization curves are calculated for the [100] and [110] directions, and these are in agreement with experiment.

THE existence of a transition in magnetite at about  $120^{\circ}\text{K}$  was evident in 1929 from the work by Weiss and Forrer<sup>1</sup> and of Millar,<sup>2</sup> who made measurements of magnetization and of specific heat, respectively. A mechanism was proposed in 1939 by Verwey,<sup>3</sup> who suggested that below the transition the  $\text{Fe}^{++}$  and  $\text{Fe}^{+++}$  ions form an ordered lattice, while at higher temperatures disorder is produced by the movement of electrons between the iron ions.

As pointed out by Verwey and de Boer,<sup>4</sup> conductivity and x-ray measurements on magnetite indicate that it has the inverse spinel structure first determined in  $\text{MgFe}_2\text{O}_4$  by Barth and Posnjak,<sup>5</sup> in magnetite eight  $\text{Fe}^{+++}$  ions occupy the tetrahedral or "A" positions, while eight  $\text{Fe}^{+++}$  and eight  $\text{Fe}^{++}$  occupy the sixteen octahedral or "B" positions in the cubic unit of structure. This has recently been confirmed by Shull, Wollan, and Koehler<sup>6</sup> using neutron diffraction. When ordering of the octahedral  $\text{Fe}^{+++}$  and  $\text{Fe}^{++}$  ions occurs at low temperatures, the structure loses its cubic symmetry. Although Verwey, Haayman, and Romeijn<sup>7</sup> described the symmetry of the proposed ordered structure as tetragonal, Bickford<sup>8</sup> pointed out that it is orthorhombic, and this has been confirmed by his own measurements<sup>9</sup> of the strains occurring during the transformation and by the x-ray measurements of Abrahams and Calhoun<sup>10</sup> ( $a=5.912$ ,  $b=5.945$ ,  $c=8.388\text{A}$ , at  $78^{\circ}\text{K}$ ). The first detection of noncubic symmetry by x-rays was by Tombs and Rooksby<sup>11</sup> who interpreted

their results as showing rhombohedral symmetry, but this appears to be inconsistent with the later x-ray work and with the results of Bickford<sup>9</sup> and of Williams and Bozorth.<sup>12</sup>

Li<sup>13</sup> first showed that the direction of easy magnetization in a single crystal below the transition temperature is influenced by the direction of the field present during the cooling through the transition. Verwey, Haayman, and Romeijn<sup>7</sup> interpreted Li's results as showing that the magnetic field caused one of the cubic axes to become the easy direction of the transformed crystal, and this interpretation has been strongly supported by Bickford's<sup>8</sup> and our results.<sup>12</sup> One of the orthorhombic axes was thus assumed to be parallel to one of the original cubic axes; the probable positions of the other axes and a method of checking them were worked out by Elizabeth A. Wood of these Laboratories and by L. R. Bickford during a discussion of the latter's strain gauge measurements and our preliminary torque measurements. The relative positions of the axes are shown in Fig. 1. This mode of transformation has now been confirmed by further measurements of Bickford<sup>9</sup> and by our present work.

Our work has been to measure the crystal anisotropy below the transition, which took place in the presence of a magnetic field oriented in various directions in the (100) and (110) planes of the crystal. (All indices refer to the original cubic axes.) The six anisotropy constants of the orthorhombic crystal were determined from the torque curves and show a high crystal anisotropy (see Fig. 7) of the same order as that deduced by Bickford<sup>14</sup> from his microwave measurements and from Domenicali's<sup>15</sup> magnetization curves. These magnetization curves, measured in the [100] and [110] directions in single crystals at low temperatures, are in accord with such curves calculated from our anisotropy constants.

\* Reported in part at the Washington Conference, September, 1952. See reference 12.

<sup>1</sup> P. Weiss and R. Forrer, *Ann. phys.* [10], **12**, 279 (1929).

<sup>2</sup> R. W. Millar, *J. Am. Chem. Soc.* **51**, 215 (1929).

<sup>3</sup> E. J. W. Verwey, *Nature* **144**, 327 (1939).

<sup>4</sup> E. J. W. Verwey and J. H. de Boer, *Rec. trav. chim.* **55**, 531 (1936).

<sup>5</sup> T. F. W. Barth and E. Posnjak, *Z. Krist.* **82**, 325 (1932).

<sup>6</sup> Shull, Wollan, and Koehler, *Phys. Rev.* **84**, 912 (1951).

<sup>7</sup> Verwey, Haayman, and Romeijn, *J. Chem. Phys.* **15**, 181 (1947).

<sup>8</sup> L. R. Bickford, *Phys. Rev.* **78**, 449 (1950).

<sup>9</sup> L. R. Bickford, *Revs. Modern Phys.* **25**, 75 (1953).

<sup>10</sup> S. C. Abrahams and B. A. Calhoun, *Acta Cryst.* **6**, 105 (1953).

<sup>11</sup> N. C. Tombs and H. P. Rooksby, *Acta Cryst.* **4**, 474 (1951).

<sup>12</sup> H. J. Williams and R. M. Bozorth, *Revs. Modern Phys.* **75**, 79 (1953).

<sup>13</sup> C. H. Li, *Phys. Rev.* **40**, 1002 (1932).

<sup>14</sup> L. R. Bickford, Laboratory for Insulation Research, Massachusetts Institute of Technology Report 23, 1949 (unpublished).

<sup>15</sup> C. A. Domenicali, *Phys. Rev.* **78**, 458 (1950).

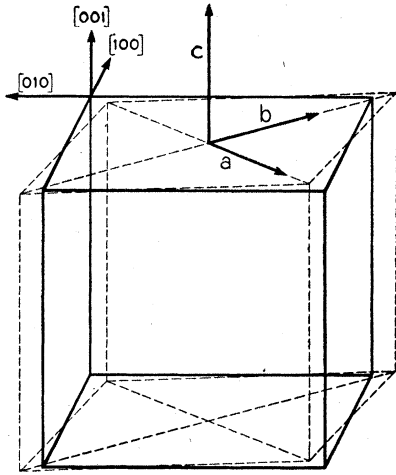


FIG. 1. Mode of transformation of cubic to orthorhombic crystal: orthorhombic  $c$  axis parallel to original cubic  $[100]$ , orthorhombic  $a$  and  $b$  axes at  $45^\circ$  to other cubic axes.

The single anisotropy constant of cubic magnetite at room temperature was also determined and compared with the value determined by Bickford<sup>8</sup> from his experiments on microwave resonance. This constant can be compared with the high coercive force observed by Gottschalk<sup>16</sup> in finely powdered material.

#### EXPRESSIONS FOR ANISOTROPY

As shown in Fig. 1, the orthorhombic  $c$  axis in  $\text{Fe}_3\text{O}_4$  is parallel to a cubic axis of the original crystal, and the  $a$  and  $b$  axes lie at about  $45^\circ$  to the cubic axes in the (001) plane. Accordingly we have chosen these orthorhombic axes to describe the magnetic anisotropy. The magnetic anisotropy energy density is then given to the second approximation by the relation

$$E = K_a \sin^2\theta_a + K_a' \sin^4\theta_a + K_b \sin^2\theta_b + K_b' \sin^4\theta_b + K_c \sin^2\theta_c + K_c' \sin^4\theta_c, \quad (1)$$

in which  $\theta_a$ ,  $\theta_b$ , and  $\theta_c$  are the angles between the direction of the saturation magnetization and the orthorhombic  $a$ ,  $b$ , and  $c$  axes, respectively. Our early results showed that three constants are not sufficient. Cross products involving two  $\theta$ 's are neglected, but their inclusion might have led to better agreement between calculated and observed torque curves. It should be pointed out that our  $a$  and  $b$  axes may be interchanged with respect to the crystallographic axes, which by convention are such that the dimensions of the unit cell are  $a < b < c$ .

When the crystal transforms on cooling there will be six possible orientations which an orthorhombic crystal may have with respect to the original crystal axes. It is assumed in our study of a natural crystal that when no field is applied during cooling, various portions transform into all of the six possible orientations. When the

crystal is heated again to room temperature, the magnetic data show that a single cubic crystal is again formed, consequently one crystal can be repeatedly cooled and heated through the transformation without deterioration.

The magnetic torque curves discussed below indicate that the direction of easy magnetization at low temperatures is the  $c$  axis. Consequently it is assumed that, when the specimen is cooled with a strong magnetic field parallel to a cubic axis, this becomes a  $c$  axis. In this case orthorhombic crystals of two orientations would be formed, corresponding to the 2 alternative positions of the  $a$  and  $b$  axes. (See the Appendix and Fig. 10.) When the cooling field is applied parallel to a cubic direction  $[110]$  there are 2 possible positions of the  $c$  axis, each with 2 positions of the  $a$  and  $b$  axes, or 4 positions in all, as shown in Fig. 11. Similarly, when the cooling field is parallel to  $[111]$  there are 6 positions to be considered, of which 3 are selected as being most probable because of energy considerations, as discussed below (see Fig. 12).

Measurements were made of the torque exerted on crystals of disk form cut parallel to (100) and (110) planes, when cooled in fields parallel to  $[001]$  in (100), and parallel to  $[001]$ ,  $[1\bar{1}0]$ , and  $[1\bar{1}1]$  in (110). The expressions for the torque under these four conditions are derived in the Appendix and are as follows, where  $H_T$  designates the field present during the cooling through the transformation and  $\theta$  is the angle measured in the given plane between the  $[001]$  direction and the saturating field used for measurement of torque:

(1)  $H_T \parallel [001]$  in (100):

$$L_1 = \frac{1}{4}(2K_a + 2K_b - 4K_c + 3K_a' + 3K_b' - 4K_c') \sin 2\theta + \frac{1}{8}(K_a' + K_b' + 4K_c') \sin 4\theta; \quad (2)$$

(2)  $H_T \parallel [001]$  in (110):

$$L_2 = (K_a - K_c + K_a' - K_c') \sin 2\theta + \frac{1}{2}(K_a' + K_c') \sin 4\theta; \quad (3)$$

(3)  $H_T \parallel [1\bar{1}0]$  in (110):

$$L_3 = \frac{1}{16}(-4K_a - 4K_b + 8K_c - 5K_a' - 5K_b' + 12K_c') \times \sin 2\theta + \frac{1}{32}(-7K_a' - 7K_b' + 4K_c') \sin 4\theta; \quad (4)$$

(4)  $H_T \parallel [1\bar{1}1]$  in (110):

$$L_4 = (4K_a - 4K_b + 3K_a' - 5K_b' + 4K_c')(\sin 2\theta)/24 + (K_a' - 7K_b' + 12K_c')(\sin 4\theta)/48 + (4K_a - 4K_b + 5K_a' - 5K_b')(\cos 2\theta)(\sqrt{2}/12) + (-K_a' + K_b')(\cos 4\theta)(\sqrt{2}/12). \quad (5)$$

These relations were used for determining the values of the 6 anisotropy constants from the data, as described below. These constants were then used for calculating torque curves for other orientations of  $H_T$ , when the symmetry does not prescribe uniquely the distribution of orthorhombic axes. For example, when  $H_T$  is applied in the (100) plane at an angle of say  $40^\circ$  to the  $[001]$

<sup>16</sup> V. H. Gottschalk, *Physics* 6, 127 (1935).

direction, it could not be predicted whether the  $c$  axes in all portions of the crystal would be parallel to  $[001]$  or whether some, on account of local fields, would be parallel to  $[010]$ . Theoretical curves can be fitted to experimental curves by assuming that a certain fraction of the specimen had  $c$  axes parallel to  $[001]$ , the remainder parallel to  $[010]$ .

Similarly torque curves were calculated for various orientations of  $H_T$  in the (110) plane. Here the positions of the  $a$  and  $b$  axes, as well as the  $c$  axes, are not generally prescribed by symmetry.

In accordance with Eq. (1), the anisotropy energies parallel to the  $a$ ,  $b$ , and  $c$  axes are

$$E_a = K_b + K_c + K_b' + K_c',$$

$$E_b = K_c + K_a + K_c' + K_a',$$

$$E_c = K_a + K_b + K_a' + K_b'.$$

Since the  $c$  axis is found to be the direction of easy magnetization, the point of zero energy is taken in this direction:

$$E_c = 0.$$

#### EXPERIMENTAL

The specimens used for most of the torque measurements were cut from a natural crystal of excellent octahedral habit obtained from the Ward Natural Science Establishment. It analyzed 71.7 percent iron, close to the theoretical 73.6 percent. A qualitative spectral analysis showed vanadium as chief impurity, present to the extent of 0.01 to 0.3 percent, and traces of other elements. Also, a specimen of artificial magnetite grown by Dr. J. Smiltens was obtained through the kindness of Professor A. von Hippel of the Massachusetts Institute of Technology. This was closely stoichiometric in composition and showed a somewhat higher anisotropy at room temperature than the natural

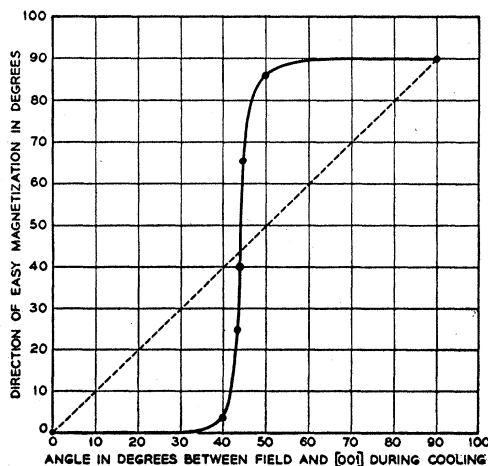


Fig. 2. (100) plane. Dependence of direction of easy magnetization on direction in which field was applied during cooling. Angles measured from  $[001]$ .

specimen. However, its magnetic anisotropy at  $-196^\circ\text{C}$  was not affected by a field of 9000 oersteds present during cooling, whereas the natural crystal was so affected.

The weight of the natural crystal disk cut in the (100) plane was 0.19 g; that cut in (110) was 0.165 g. The ratios of diameter to thickness were, respectively, 4.6 and 2.5. Measurement of the torque was carried out in the apparatus designed by Williams,<sup>17</sup> which could be read to 5 dyne-cm, corresponding to an anisotropy energy of 500 to 1000 erg/cm<sup>3</sup> in the specimens used. Field strengths of 9000 oersteds were used for measurement, and this was sufficiently high so that no correction was needed for the torque at saturation.

The specimen was imbedded in a brass disk and fixed in position by placing Scotch tape on it under slight pressure. This was placed in a Lucite cup, which was kept filled with liquid nitrogen for cooling through the transition and for measurement. The orientations of the crystals were first determined by x-rays, and later the directions of easy magnetization at room temperature were taken as  $[011]$  in (100) and  $[\bar{1}11]$  in (110). As noted by Okamura and Ogawa,<sup>18</sup> the direction of easy magnetization shifts from  $[\bar{1}11]$  to  $[100]$  just above the transition point near  $-140^\circ\text{C}$ , on cooling. This observation was used by Bickford<sup>8</sup> to explain the maximum in the curve of  $\mu_0$  vs temperature reported by Snoek<sup>19</sup> at about this temperature.

Torque curves were taken at room temperature, and at  $-196^\circ\text{C}$  after cooling in zero field or in a field of 9000 oersteds in various directions in the plane of the specimen.

#### RESULTS

The torque curves at room temperature, for the (100) and (110) disks of the natural crystal, and the (110) artificial crystal, yielded the following values of the cubic anisotropy constant  $K$ :  $-140\,000$ ,  $-140\,000$ , and  $-127\,000$  ergs/cm<sup>3</sup>, respectively. This may be compared with the average value  $-112\,000$  derived by Bickford<sup>8</sup> from his microwave resonance measurements of several natural and artificial crystals. His lower values may be due to the fact that the field present during measurement was not sufficient to saturate, or the values for our natural crystal may be the result of the impurities it contains.

The effect of the direction of the field present during cooling on the resulting direction of easy magnetization, subsequently measured at  $-196^\circ\text{C}$ , is shown for the (100) disk in Fig. 2. This shows that the easy direction coincides with that direction of the  $\langle 100 \rangle$  form, namely  $[001]$ , that is nearest to the direction of the field, until these two directions differ by about  $40^\circ$ . Apparently

<sup>17</sup> See R. M. Bozorth, *Ferromagnetism* (D. Van Nostrand Company, New York, 1951), p. 556 and 831.

<sup>18</sup> T. Okamura and S. Ogawa, *Proc. Phys.-Math. Soc. Japan* 23, 363 (1941).

<sup>19</sup> J. L. Snoek, *New Developments in Magnetic Materials* (Elsevier Publishing Company, Inc., New York, 1947), p. 25.

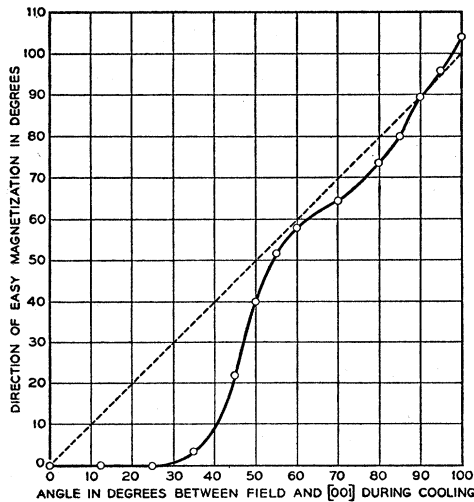


FIG. 3. (110) plane. Dependence of direction of easy magnetization on direction of field during cooling. Angles measured from [001].

some portions of the specimen then begin to have easy directions in the next-nearest  $\langle 100 \rangle$  direction, [010], and the portions become about equal when the angle is  $45^\circ$ , as is to be expected. This supports the idea that the orthorhombic  $c$  axis, which is parallel to one of the original cubic axes, is the direction of easiest magnetization in the orthorhombic crystal.

Similar data for the (110) plane (Fig. 3) show that deviations of the easy direction from the nearest  $\langle 100 \rangle$  direction occur when this direction is only about  $30^\circ$ , considerably less than the angle for the first deviation

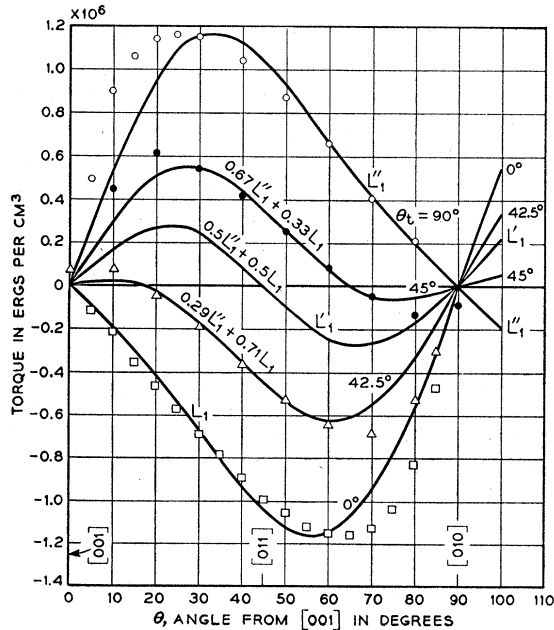


FIG. 4. Torque curves for (100) plane, obtained after cooling with magnetic field inclined at various angles  $\theta_T$  to [001] direction. Points show experimental values, lines are theoretical curves.

in the (100) plane. When the angle between  $H_T$  and [001],  $\theta_T$ , reaches  $55^\circ$ , the  $c$  axes should be equally distributed along the 3 original cubic axes and the easy direction of the crystal, represented by  $\theta_E$ , should be parallel to  $\theta_T$ . They are observed to be parallel within about  $3^\circ$ . Between  $\theta_T = 55^\circ$  and  $90^\circ$ ,  $\theta_E$  may be expected to be less than  $\theta_T$ , and at  $\theta_T = 90^\circ$   $\theta_E$  should equal  $\theta_T$ , as observed. At  $\theta_T = 90^\circ$  the easy direction is expected to become greater than  $\theta_E$ , as observed, and the curve should continue symmetrically.

Torque curves for the (100) and (110) planes, measured after cooling in fields inclined at various angles to [001], are shown in Figs. 4, 5, and 6. The torque curve for the (110) specimen cooled in a field parallel to the [001] direction ( $\theta_T = 0$ ) should be especially noted. When measurements were made up to about  $\theta = 40^\circ$ , they were quite reproducible, but beyond this point the torque was found to decrease with time. After  $\theta$  was increased slowly to  $90^\circ$ , allowing time for this drift to complete itself, the curve was again measured and was now completely reproducible over its entire extent, at a level considerably below the original one. It is believed that this is due to the shift, in the high applied field used during measurement, of those  $a$  axes which are originally at  $90^\circ$  to the (110) plane, to the alternative position lying in the plane, the related  $b$  axes shifting in the opposite sense. This orientation is energetically more favorable, as shown in Fig. 7, and is that considered in the Appendix, Case 2. Such a shift has also been noted by Bickford,<sup>8</sup> who found that in one of his specimens a field applied below the transition can switch a magnetic axis from one cubic axis to another.

#### DERIVATION OF CONSTANTS

The anisotropy constants,  $K_a$  to  $K_c'$ , were derived from the following torque curves:

- (100) plane,  $H_T \parallel [001]$  (Fig. 4),
- (110) plane,  $H_T \parallel [001]$  (Fig. 5),
- (110) plane,  $H_T \parallel [1\bar{1}0]$  (Fig. 6),
- (110) plane,  $H_T \parallel [1\bar{1}1]$  (Fig. 5),

using the expressions for  $L_1$  to  $L_4$  [Eqs. (2)–(5)] and the additional expression

$$E_c = K_a + K_b + K_a' + K_b' = 0.$$

These curves were fitted to the data at  $\theta = 30^\circ$  and  $\theta = 60^\circ$  for  $L_1$ ,  $L_2$ , and  $L_3$ , and  $\theta = 30^\circ$ ,  $60^\circ$ , and  $90^\circ$  for  $L_4$ . With the further condition  $E_c = 0$  we then had 10 relations from which the six constants were derived using the method of least squares. The derived constants are, in ergs/cm<sup>3</sup>,

$$\begin{array}{ll} K_a: & 890 \times 10^3, & K_a': & -400 \times 10^3, \\ K_b: & -620 \times 10^3, & K_b': & 120 \times 10^3, \\ K_c: & 370 \times 10^3, & K_c': & 620 \times 10^3; \end{array}$$

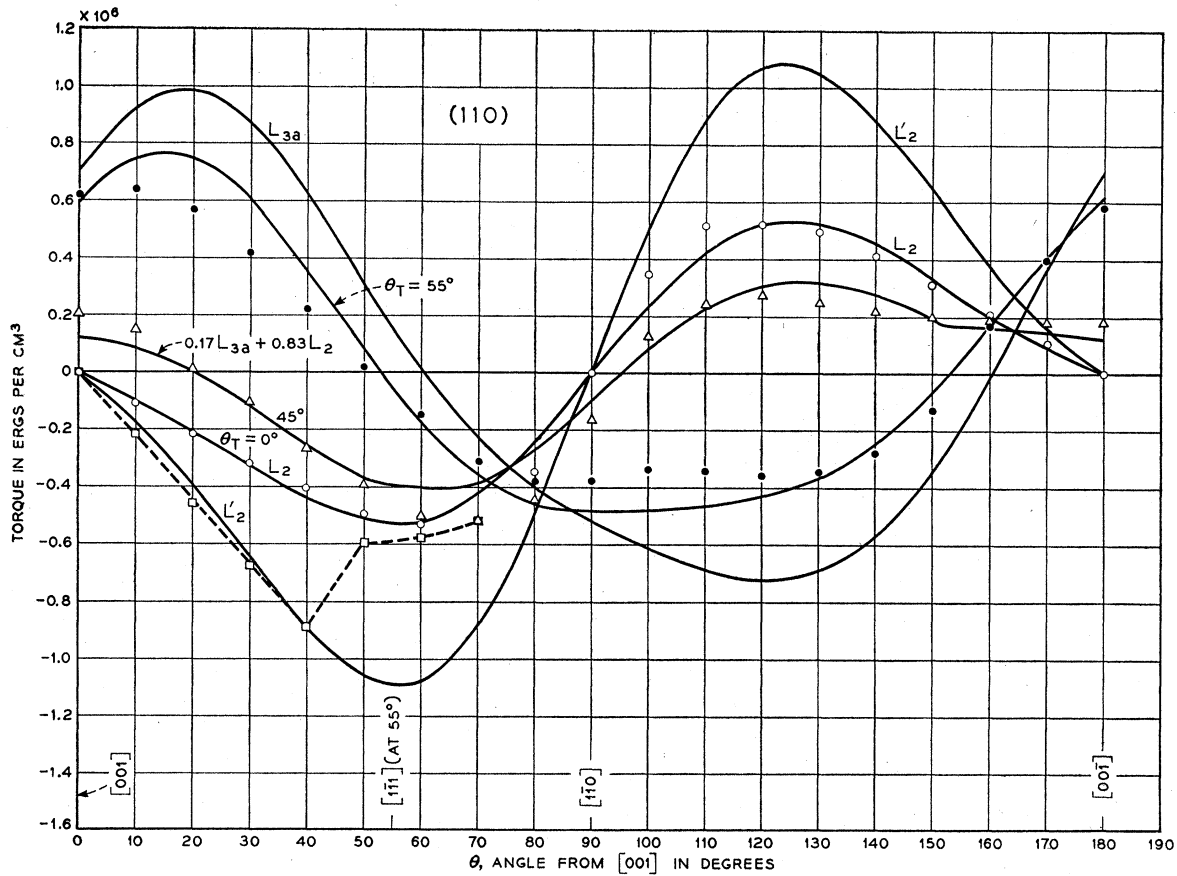


FIG. 5. Torque curves for (110) plane with cooling field applied at 0°, 45°, and 55° from [001]. Curves for 45° and 55° are combinations of  $L_2$  and  $L_{3a}$  in different proportions (see text).

and the anisotropy energies parallel to the  $a$ ,  $b$ , and  $c$  axes are, in ergs/cm<sup>3</sup>,

$$E_a = 490 \times 10^3, \quad E_b = 1490 \times 10^3, \quad E_c = 0.$$

The accuracy of the constants is not high—the probable error averages about  $100 \times 10^3$ ,

The torque curves  $L_1$  to  $L_4$  were then calculated from the anisotropy constants and compared with the experimental curves. This comparison is shown in Figs. 4 to 6. There is some evidence that agreement would be improved slightly by the addition of a  $6\theta$  term that would come from higher terms in the expansion of  $E$  [Eq. (1)]. However, no attempt was made to improve the fit in this manner.

The torque curves obtained after cooling with  $H_T$  making various other angles to the axes were also calculated from the  $K$ 's and compared with experiment, as shown in the same figures. These curves all have shapes that are accounted for by theory, and they are in fair quantitative agreement with the values of the  $K$ 's selected.

In several cases the theory does not predict the fractions of the crystal that have transformed in two ways; in these cases curves can be fitted by assuming

arbitrary fractions transformed in one way, the remaining transforming the alternate way. For example,

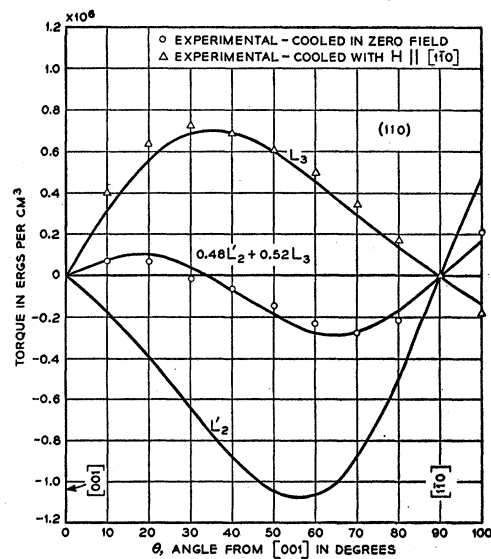


FIG. 6. Additional theoretical torque curves and observed points for (110) plane.

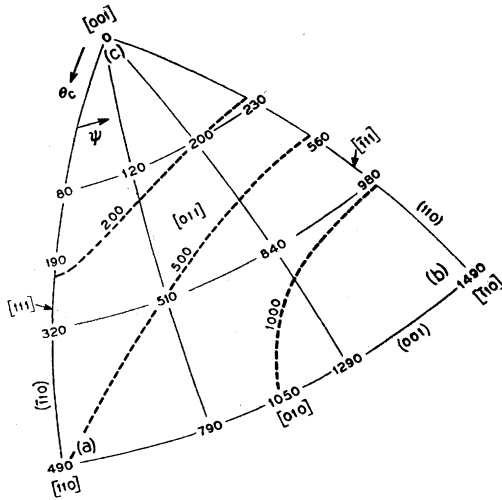


FIG. 7. Anisotropy energies, in  $10^8$  ergs/cm $^3$ , in various directions in transformed orthorhombic crystal. Note both orthorhombic axes ( $a$ ,  $b$ ,  $c$ ) and original cubic axes ( $[100]$ , etc.).

when  $H_T$  is applied  $42.5^\circ$  from  $[001]$  in  $(100)$ , the experimental torque curve can be satisfied by assuming that in 71 percent of the specimen the  $c$  axis lies along  $[001]$  and in 29 percent along  $[010]$ , as shown in Fig. 4. This distribution is probably caused by the local variations in the direction of the internal field, caused by local strains and imperfections.

In the  $(110)$  plane, with  $\theta_T = 45^\circ$ , the crystals transform so that the resultant torque curve is a combination of  $L_2$  and  $L_{3a}$ , as shown in Fig. 5 and discussed in the Appendix. When  $\theta_T > 60^\circ$  it appears that a third orientation is possible—that corresponding to  $L_3$ . When  $\theta_T = 80^\circ$  the direction of easy magnetization lies at  $\theta = 65^\circ$ ; by combining  $L_2$ ,  $L_3$ , and  $L_{3a}$  the observed easy directions lying between  $\theta = 60^\circ$  and  $90^\circ$  can thus be accounted for, and at  $90^\circ$  all portions of the crystal transform in accordance with  $L_3$  of Fig. 6.

The torque curves measured in the  $(100)$  plane after cooling in zero field were found to be somewhat different in different experiments, perhaps because the crystal was not properly demagnetized before cooling. They agree with the theoretical expression  $L_{100}$  (Appendix, Case 5) in general character; the  $\langle 110 \rangle$  are the easy and the  $\langle 100 \rangle$  the hard directions in this plane, and the average amplitude is very close to that calculated from the constants  $K_a, \dots, K_c'$ , namely,  $230 \times 10^8$  ergs/cm $^3$ . It is at first thought surprising but is in accord with theory that a  $\langle 100 \rangle$  direction, which in a single oriented orthorhombic crystal can become the easiest direction of all, will be the hard direction when all possible orientations are present.

The torque curve in the  $(110)$  plane after cooling in zero field also shows, in agreement with theory, that  $[001]$  is not as easy a direction as  $[1\bar{1}1]$ . The observed curve is not in agreement with equal distribution of the  $c$  axes among the three possible  $\langle 100 \rangle$  directions, but

indicates, as shown in Fig. 6, that 48 percent instead of 33 percent of the  $c$  axes lie parallel to  $[001]$ . This may also be due to imperfect demagnetization.

The anisotropy energies in various directions in the orthorhombic crystal are shown in Fig. 7. The highest energy, along the  $b$  axis, is  $1.5 \times 10^6$  ergs/cm $^3$ .

### MAGNETIZATION CURVES

Domenicali<sup>15</sup> has measured the magnetization curves at  $-180^\circ\text{C}$  for crystals cooled in zero field and magnetized in the  $[100]$  and  $[110]$  directions. These curves

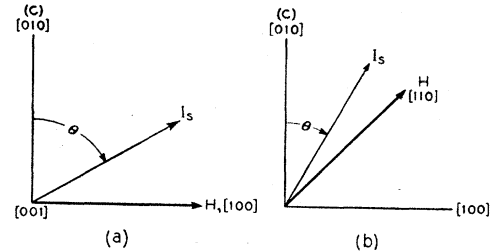


FIG. 8. Diagram for calculating magnetization curves from anisotropy energies: (a)  $H \parallel [100]$ , drawing magnetization  $I_s$  from direction of easy magnetization  $[010]$ ; (b)  $H \parallel [110]$ .

can be calculated theoretically from our constants as follows: One-third of the crystal will transform with its  $c$  axis parallel or antiparallel to  $[100]$ . When the measuring field is applied parallel to  $[100]$  only a weak field, assumed to be negligible, will be required to orient its moment parallel to the field. In the other  $\frac{2}{3}$  of the crystal the  $c$  axis will lie at  $90^\circ$  to the applied field  $H$ , and the spontaneous magnetization  $I_s$  will gradually be rotated from the  $c$  axis into the direction of  $H$  as its strength increases. The energy of anisotropy  $E$  plus the mutual magnetic energy between  $H$  and  $I_s$  is then

$$E_T = E - HI_s \sin\theta,$$

$\theta$  being defined as in Fig. 8(a). This is a minimum when  $\partial E_T / \partial \theta = 0$ , or, since  $L = -\partial E / \partial \theta$ , we have

$$H = -L / (I_s \cos\theta).$$

The intensity of magnetization is

$$I_1 = I_s \sin\theta.$$

In this case  $L = L_1$  [Eq. (2) above]; this is an approximation only, for  $I_s$  may not be exactly in a  $(100)$  plane. For the crystal as a whole,

$$I_{100} = I_s/3 + 2I_1/3,$$

and  $I$  is easily calculated as  $f(H)$ .

When  $H$  is applied parallel to  $[110]$ ,  $H$  is inclined to the  $c$  axis by  $45^\circ$  for  $\frac{2}{3}$  of the crystal, by  $90^\circ$  for  $\frac{1}{3}$  of it. For  $\frac{2}{3}$  of the crystal [see Fig. 8(b)],

$$H_1 = -L_1 / [I_s \sin(\frac{1}{2}\pi - \theta)],$$

$$I_1' = I_s \cos(\frac{1}{2}\pi - \theta).$$

For the other  $\frac{1}{3}$  of the crystal we have [Fig. 8(a)]

$$H_2 = -L_2 / (I_s \cos\theta),$$

and

$$I_2 = I_s \sin\theta.$$

The resultant curve for the whole crystal is then readily determined by evaluating  $I_{110} = I_2/3 + 2I_1'/3$  for given values of  $H = H_1 = H_2$ .

The demagnetizing factor  $N$  for Domenicali's disk-shaped specimen can be calculated approximately from the dimensions, which have a ratio of length to thickness of 5. Using  $N = 1.54$  and  $I_s = 500$ , the demagnetizing fields were added to the fields calculated above. The resultant  $I, H$  curves are compared with Domenicali's measurements for  $-180^\circ\text{C}$  in Fig. 9. Considering the fact that the anisotropy constants are those determined for  $-196^\circ\text{C}$  and that hysteresis is not taken into account, the agreement is good.

The magnetization of finely powdered magnetite at low temperature will take place entirely by domain rotation and not by boundary movement, and the coercive force can be calculated. If the magnetizing field is applied always parallel to the  $c$  axis, reversal of magnetization will take place by rotation of the magnetization vector in the (110) plane through the direction of the  $a$  axis, over an energy hump of  $0.5 \times 10^6$  ergs/cm<sup>3</sup>. To obtain the field necessary for this reversal,

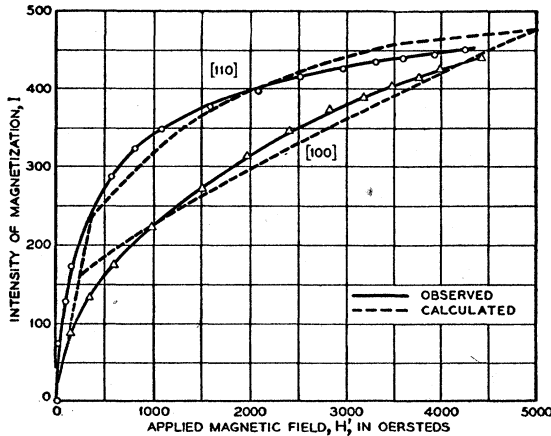


FIG. 9. Calculated magnetization curves for [001] and [110] directions at  $-195^\circ\text{C}$  (broken lines) compared with Domenicali's observed curves (solid lines).

$-L_2$  is equated to the torque created by the applied field:

$$HI_s \sin\theta = -(K_a - K_c + K_a' - K_c') \sin 2\theta - \frac{1}{2}(K_a' + K_c') \sin 2\theta.$$

The largest value of  $H$  for the various values of  $\theta$ , in this case the value for  $\theta = 41^\circ$ , is the coercive force. We obtain

$$H_c = 1420 \text{ oersteds.}$$

No measurements of coercive force at this temperature have been reported for fine particles.

Similarly the coercive force of fine powder at room temperature may be calculated from the cubic anisotropy constant  $K$ . When crystals are oriented at random with respect to the magnetizing field we have<sup>17</sup>

$$H_c = 0.64 |K| / I_s \approx 160.$$

This is to be compared with the highest observed value of Gottschalk, 127 oersteds, in particles ground to about 4-microns diameter. This particle size is rather large to show the fine-particle effect; it is possible that the particles observed are agglomerates of finer particles, or that they are under enough strain to account for the high coercive force.

We are glad to acknowledge the benefit of discussions with Dr. R. W. Hamming and Dr. J. W. Tukey on the evaluation of the constants. The derivations of the equations were checked by Miss B. B. Cetlin, and the calculations of the constants by least squares were carried out under the supervision of Miss C. L. Froelich, to whom we are indebted.

#### APPENDIX

*Case 1:* A disk cut parallel to a (100) plane is cooled in a field,  $H_T$ , parallel to the [001] direction lying in the plane. It is assumed that the orthorhombic  $c$  axis will be parallel to [001], the  $a$  and  $b$  axes inclined  $45^\circ$  to the plane. See Fig. 10. Let  $\theta$  be the angle in the plane between the [001] direction and the direction of the field,  $H_m$ , applied during measurement. Then [see Eq. (1)]  $\theta_c = \theta$ ,  $\cos\theta_b = \cos\theta_a = (\sin\theta)/\sqrt{2}$  and the anisotropy energy is

$$E_1 = \frac{1}{4}(3K_a + 3K_b + 2K_c) + \frac{1}{32}(19K_a' + 19K_b' + 12K_c') + \frac{1}{8}(2K_a + 2K_b - 4K_c + 3K_a' + 3K_b' - 4K_c') \cos 2\theta + \frac{1}{32}(K_a' + K_b' + 4K_c') \cos 4\theta.$$

The torque in the plane,  $L_1 = -\partial E / \partial \theta$ , is given by Eq. (2) in the text. Since the  $a$  and  $b$  axes make the same angle with  $H_m$ , the torque on the two crystal

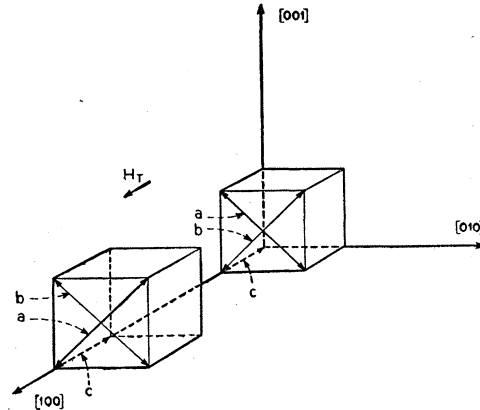


FIG. 10. Possible orientations of orthorhombic crystals resulting from cooling cubic crystal in field parallel to [100].

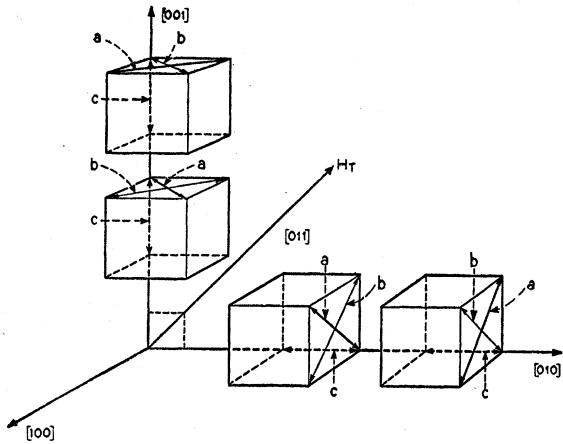


FIG. 11. Orientations of orthorhombic crystals when cooling field is parallel to  $[110]$ .

positions (those with  $a$  and  $b$  axis interchanged) is the same.

When  $H_T$  is parallel to  $[011]$ , it is assumed that the  $c$  axes are equally distributed between  $[001]$  and  $[010]$ . For half the crystal the torque is given by  $L_1$  above, and for the other half  $\theta$  is replaced by  $(\theta + \frac{1}{2}\pi)$  so that  $L_1''(\theta) = L_1(\theta + \frac{1}{2}\pi)$  as in Fig. 4. The sum of the two is then  $\frac{1}{2}[L_1(\theta) + L_1(\theta + \frac{1}{2}\pi)]$  or  $L_1' = \frac{1}{8}(K_a' + K_b' + 4K_c') \times \sin 4\theta$ . This relation contains the same coefficient of  $\sin 4\theta$  as we have in  $L_1$ , but now the coefficient of  $\sin 2\theta$  is zero.

*Case 2:* The disk is cut parallel to  $(110)$  and cooled with  $H_T$  parallel to  $[001]$ , and  $\theta$  is measured in the plane from  $[001]$ . It is assumed that all portions of the crystal have  $c$  axes parallel to  $[001]$  and that just after cooling in half of the crystal the  $a$  axes lie in the  $(110)$  plane along  $[1\bar{1}0]$ , and in half the  $a$  axes are  $90^\circ$  to the plane, along  $[110]$ , the  $b$  axes lying in the alternate positions. See Fig. 10. Experiments indicate, however, that after applying a strong field at  $\theta = 40^\circ$  to  $90^\circ$  a rearrangement of axes takes place, and it is assumed that thereafter the  $a$  axes lie in the  $(110)$  plane throughout the crystal, the  $c$  axes remaining as before. For this case  $\theta_c = \theta$ ,  $\theta_b = \pi/2$  and  $\theta_a = \pi/2 - \theta$ . Then

$$E_2 = \frac{1}{2}(K_a + 2K_b + K_c) + \frac{1}{8}(3K_a' + 4K_b' + 3K_c') \\ + \frac{1}{2}(K_a - K_c + K_a' + K_c') \cos 2\theta + \frac{1}{8}(K_a' + K_c') \cos 4\theta,$$

and  $L_2$  is given by Eq. (3) in the text. In the former case, with two orientations of crystals present, we must calculate the torque when the  $b$  axes lie in the plane. Now  $\theta_c = \theta$ ,  $\theta_b = \frac{1}{2}\pi - \theta$ , and  $\theta_a = \frac{1}{2}\pi$ . The torque is

$$L_{2a} = (K_b - K_c + K_b' - K_c') \sin 2\theta + \frac{1}{2}(K_b' + K_c') \sin 4\theta,$$

and the torque for equal proportions of the two crystal orientations is

$$L_2' = \frac{1}{2}(L_2 + L_{2a}) = \frac{1}{2}(K_a + K_b - 2K_c + K_a' + K_b' - 2K_c') \\ \times \sin 2\theta + \frac{1}{4}(K_a' + K_b' + 2K_c') \sin 4\theta.$$

*Case 3:* When  $H_T$  is applied parallel to  $[1\bar{1}0]$  in the  $(110)$  disk, the  $c$  axes are inclined  $45^\circ$  to the plane and to  $H_T$ , half above and half below ( $[100]$  and  $[010]$ ). Since each portion has the same torque we need calculate it only for one case; however, each  $c$  axis position is accompanied by two possible arrangements of  $a$  and  $b$  axes as shown in Fig. 11. In the one case, measuring  $\theta$  from  $[001]$ , we have  $\cos \theta_a = (\sin \theta)/2 + (\cos \theta)/\sqrt{2}$ ,  $\cos \theta_b = (\sin \theta)/2 - (\cos \theta)/\sqrt{2}$ ,  $\cos \theta_c = (\sin \theta)/\sqrt{2}$ , and

$$E_{3a} = \frac{1}{8}(5K_a + 5K_b + 6K_c) + (1/64)(15K_a' + 15K_b' + 11K_c') \\ + \frac{1}{32}(-4K_a - 4K_b + 8K_c - 5K_a' - 5K_b' + 12K_c') \cos 2\theta \\ + (-4K_a + 4K_b - 5K_a' + 5K_b')(\sin 2\theta)/8\sqrt{2} \\ + (-7K_a' - 7K_b' + 4K_c')(\cos 4\theta)/128 \\ + (K_a' - K_b')(\sin 4\theta)/16\sqrt{2},$$

and

$$L_{3a} = (-4K_a - 4K_b + 8K_c - 5K_a' \\ - 5K_b' + 12K_c')(\sin 2\theta)/16 \\ + (4K_a - 4K_b + 5K_a' - 5K_b')(\cos 2\theta)/4\sqrt{2} \\ + (-7K_a' - 7K_b' + 4K_c')(\sin 4\theta)/32 \\ + (-K_a' + K_b')(\cos 4\theta)/4\sqrt{2}.$$

For the second position,  $L_{3b}$  is given by interchanging subscripts  $a$  and  $b$  in  $L_{3a}$ . Then  $L_3 = \frac{1}{2}(L_{3a} + L_{3b})$  and is given by Eq. (4) in the text.

*Case 4:* When  $H_T$  is applied parallel to  $[1\bar{1}1]$  in  $(110)$ , the  $c$  axes lie along original cubic axes, and so we have 3 possible positions, each equally inclined to  $H_T$ . However, each position of the  $c$  axis has 2 possible positions for its corresponding  $a$  and  $b$  axes. Of these the  $a$  axis is a direction of lower energy; therefore it is assumed that it will be oriented more nearly in the direction of the field used during cooling, as shown in Fig. 12. When the  $c$  axis lies in the plane of the disk, the  $a$  axes will also lie in the plane of the disk and the  $b$  axes perpendicular thereto. Then  $\frac{1}{3}$  of the crystal has the torque  $L_2$  and  $\frac{2}{3}$  of the crystal the torque  $L_{3a}$  given above. The whole

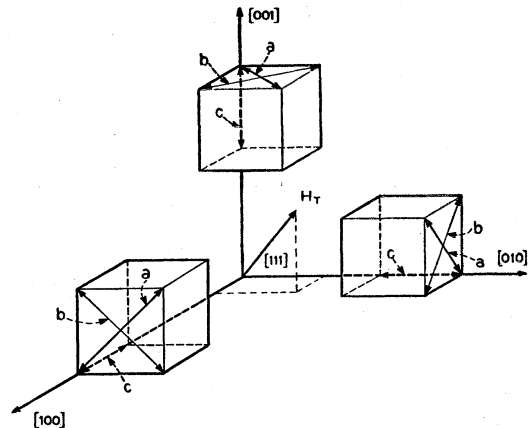


FIG. 12. Orientations of orthorhombic crystals when cooling field is parallel to  $[111]$ .

torque is then

$$L_4 = \frac{1}{3}L_2 + \frac{2}{3}L_{3a},$$

given in Eq. (5) in the text. In this case, for the first time, cosine terms are present and the calculated and observed torque curves are less symmetrical—in the  $0^\circ$  to  $180^\circ$  range in  $\theta$  no symmetry is present. In general  $L \neq 0$  at  $\theta = 0$ .

*Case 5:* When no field is applied during cooling, the torque for the (100) plane is calculated in three parts, corresponding to three positions of the  $c$  axis: (1) regions having  $c$  axes parallel to  $[001]$ , (2) regions having  $c$  axes parallel to  $[010]$ , and (3) regions having  $c$  axes parallel to  $[100]$ , perpendicular to the plane of measurement. The torque for the first 2 positions combined is described by  $L_1'$  (Case 1 of Appendix). For the third position there are two possible orientations of the  $a$  and  $b$  axes,  $90^\circ$  to each other in the (100) plane; for one of these  $\theta_c = 90^\circ$ ,  $\theta_b = \frac{1}{4}\pi + \theta$ ,  $\theta_a = \frac{1}{4}\pi - \theta$ , and the corre-

sponding energy and torque are

$$E_{5a} = \frac{1}{2}(K_a + K_b + 2K_c) + \frac{1}{8}(3K_a' + 3K_b' + 8K_c') \\ + \frac{1}{2}(-K_a + K_b - K_a' + K_b') \sin 2\theta - \frac{1}{8}(K_a' + K_b') \cos 4\theta$$

and

$$L_{5a} = (K_a - K_b + K_a' - K_b') \cos 2\theta - \frac{1}{2}(K_a' + K_b') \sin 4\theta.$$

The energy, and torque  $L_{5b}$ , for the other orientation of position (3) are obtained by interchanging subscripts  $a$  and  $b$  in these expressions.

The result is then

$$L_{100} = \frac{1}{6}(4L_1' + L_{5a} + L_{5b}) = -\frac{1}{2}(K_a' + K_b' - 4K_c') \sin 4\theta.$$

*Case 6:* When no field is applied to the (110) specimen during cooling,  $\frac{1}{3}$  of the specimen will have the torque  $L_2'$  (Case 2 above),  $\frac{2}{3}$  will have  $L_3$  (Case 3 above):

$$L_{110} = \frac{1}{3}(L_2 + 2L_3) = \frac{1}{3}(-K_a' - K_b' + 4K_c')(\sin 2\theta)/24 \\ + \frac{1}{3}(-3K_a' - 3K_b' + 8K_c')(\sin 4\theta)/48.$$

## Deformation of Copper Single Crystals at 300°K and 78°K

T. H. BLEWITT

*Oak Ridge National Laboratory, Oak Ridge, Tennessee*

(Received April 20, 1953)

Single crystals of copper were deformed at 78°K and 300°K. There was slight temperature dependence of the critical shear stress in this range of temperature and for shear strains less than about 0.25 the stress-strain relationship was linear and independent of temperature. The linear relationship of the stress-strain curve persisted for higher strains at 78°K. The annealing at 300°K of crystals deformed at 78°K showed a decrease in electrical resistance accompanied by a phenomenon suggestive of strain aging. The magnitude of the recoverable resistance was dependent on the strain varying at a faster rate than a linear relationship. A measurable decrease in electrical resistance was not observed for strains less than about 0.30. These results are interpreted according to the theory of dislocations and indicate some modification to the theory of work hardening suggested by Mott.

### I. INTRODUCTION

THERE has recently been considerable interest in the phenomena of low-temperature annealing of the electrical resistivity in cold-worked metals. The motivation for this work originates in an interesting paper presented by Seitz<sup>1</sup> at the Pittsburgh Conference on Plastic Deformation, in which Seitz pointed out that plastic deformation increased the number of vacant lattice sites in ionic crystals by about a hundredfold. He also pointed out that after about one hour at room temperature, the number of vacancies has decreased to the equilibrium number. Shortly thereafter a group of experimentalists at North American Aviation<sup>2</sup> found that metals, specifically copper and aluminum, irradiated by 36-Mev  $\alpha$  particles at  $-160^\circ\text{C}$  in the Berkeley

cyclotron showed an apparent decrease in residual resistance on warming to room temperature. Since theoretical studies of Seitz<sup>3</sup> and others had indicated that vacant lattice sites and interstitial atoms should be formed by the bombardment of metals by high energy particles, the annealing effects observed by the North American Aviation, and more recently by a group at Illinois,<sup>4</sup> might be attributed to the movement of these defects. Thus, if metals showed a behavior similar to that observed by ionic crystals in that lattice vacancies or interstitial atoms were formed by plastic deformation then an annealing phenomenon in cold-worked metals similar to that observed in irradiated metals should be observed. With this in mind a group at Oak Ridge National Laboratory<sup>5</sup> made measurements on the effect of a room temperature warmup on the elec-

<sup>1</sup> F. Seitz, *Pittsburgh Conference on Plastic Deformation of Crystalline Solids, May, 1950*, U. S. Office of Naval Research Report NAVEXOS-P-834 (unpublished), p. 37

<sup>2</sup> Eggleston, Martin, and Tarpinian, *Phys. Rev.* **81**, 664 (1951).

<sup>3</sup> F. Seitz, *Disc. Faraday Soc.* No. 5, 271 (1949).

<sup>4</sup> Marx, Copper, and Henderson, *Phys. Rev.* **88**, 1006 (1952).

<sup>5</sup> Blewitt, Taylor, and Coltman, *Phys. Rev.* **82**, 769 (1951).